J. Phys. B: At. Mol. Opt. Phys. **31** (1998) 2077–2090. Printed in the UK PII: S0953-4075(98)89601-6

On the calculation of electron-impact rotational excitation cross sections for molecular ions

Ismanuel Rabadán†, Baljit K Sarpal‡ and Jonathan Tennyson†§

† Department of Physics and Astronomy, University College London, Gower Street, London WC1E 6BT, UK

‡ Department of Physics, The University of Newcastle upon Tyne, Newcastle upon Tyne, NE1 7RU, UK

Received 28 November 1997, in final form 5 February 1998

Abstract. Methods of computing rotational excitation cross sections for electron collisions with diatomic molecular ions are examined for impact energies up to 5 eV. The HeH^+ and NO^+ ions are used as test cases and calculations are performed at various levels of approximation. Previous studies have all used the Coulomb–Born approximation assuming only dipolar potentials. This approximation is found to be unreliable in a number of aspects: short-range and threshold effects are important, and the widely made assumption that only $\Delta j = 1$ processes need to be considered is particularly questionable. Conversely, full inclusion of vibrational motion is found to be less important.

1. Introduction

The very large cross sections found for collisions between electrons and molecular ions mean that such collisions can have a significant effect on the molecular ion population even at low electron densities. For example, in diffuse molecular plasmas, such as those found in a number of astronomical environments, electron-impact excitation is thought to directly determine the radiative properties of the molecular ions (Neufeld and Dalgarno 1994). Thus, for example, the strength of the HeH^+ $j = 1 \rightarrow 0$ transition which should be observable in planetary nebulae, such as NGC 7027, is thought to be directly proportional to the electron-impact rotational excitation cross section of HeH^+ (Roberge and Dalgarno 1982, Cecchi-Pestellini and Dalgarno 1993). Similar arguments can be made for other molecular ions such as CH^+. However, recent observations of CH^+ in states up to $j = 6$ (Cernicharo *et al* 1997) and attempts to detect HeH^+ (Liu *et al* 1997) have prompted us to examine the reliability of the available data for this process, all of which is theoretical.

Methods of calculating rotational excitation parameters for electron collisions with neutral molecules have been studied in considerable detail (Morrison and Sun 1995). However, for molecular ions, nearly all rotational excitation calculations appear to have been performed within the Coulomb–Born (CB) approximation, for example Chu (1975), Dickinson and Muñoz (1977), Flower (1979), Dickinson and Flower (1981), Neufeld and Dalgarno (1994). This approximation assumes that only long-range electron–molecule interactions need be considered. All previous applications of the CB approximation assumed that this long-range interaction is purely dipolar. Within this model, collisions can only change the rotational quantum number of the molecular ion, j, by one.

§ E-mail address: j.tennyson@ucl.ac.uk

0953-4075/98/092077+14$19.50

In this paper we compare results obtained within the (dipole and quadrapole) CB approximation with more sophisticated models based on a full treatment of the interactions. In particular, we probe the effect of short-range interactions, vibrational motion and explicit allowance for rotational thresholds on the calculated cross sections. We also consider collisions for which $\Delta j > 1$.

Clearly the most comprehensive treatment of rotational excitation is given by full rotational close coupling. Such calculations have been performed for ultra-low-energy collisions between electrons and neutral diatomics (Thümmel *et al* 1993). However, the plasma data are necessary for electron temperatures up to about 10 000 K, which in turn means that rates are sensitive to collision energies up to 5 eV. At these energies methods based on rotational close coupling are impractical due to the excessively large number of channels that would need to be considered. In this work, therefore, we restrict our comparisons to methods based on frame transformations (Lane 1980) with possible corrections for thresholds artefacts of this model (Chandra and Temkin 1976).

In the next section we present the various theoretical approaches to the rotational excitation problem that we test here. To test these models, calculations are performed for two diatomic ions: the light and strongly dipolar HeH^+, and the heavier NO^+, which is often described as quadrupole dominated. Section 3 describes the various e^-–HeH^+ and e^-–NO^+ wavefunctions employed. Sections 4 presents our results and discussion. Major conclusions are summarized in section 5.

2. Theory

2.1. Coulomb–Born approximation

In this work we follow the implementation of the CB approximation for the study of rotational excitation of molecular (linear) ions by electron impact of Chu and Dalgarno (1974). This, in turn, was based on work by Alder *et al* (1956) on nuclear structure.

We are interested in the process:

$$e^-(k_i) + \mathrm{ION}(j, m) \rightarrow e^-(k_f) + \mathrm{ION}(j', m')$$

where j and m are the rotational and projection quantum numbers of the linear, rigid rotor ION, and k_i (k_f) the initial (final) momentum of the electron:

$$k_i = \sqrt{2E_i} \qquad (1)$$
$$k_f = \sqrt{2\{E_i + B_e[j(j+1) - j'(j'+1)]\}}$$

where E_i is the initial energy of the projectile and B_e is the rotational constant of ION.

Within the CB approximation, the cross section for the rotational excitations, averaging in m and summing in m', is (Chu and Dalgarno 1974)

$$\sigma^{\mathrm{CB}}(j \rightarrow j') = \sum_{\lambda=1}^{\infty} \sigma_\lambda^{\mathrm{CB}} \qquad (2)$$

with

$$\sigma_\lambda^{\mathrm{CB}}(j \rightarrow j') = 16\pi \frac{k_f}{k_i} Q_\lambda^2 \frac{2j'+1}{2\lambda+1} \begin{pmatrix} j & j' & \lambda \\ 0 & 0 & 0 \end{pmatrix} \times \sum_{l_i l_f} (2l_i+1)(2l_f+1) \begin{pmatrix} l_i & l_f & \lambda \\ 0 & 0 & 0 \end{pmatrix}^2 \left| M_{l_i,l_f}^{-\lambda-1} \right|^2 \qquad (3)$$

where Q_λ is the λth permanent electric moment of ION, the $(\cdots)$ are the usual $3j$ symbols and $M_{l_i,l_f}^{-\lambda-1}$ are radial matrix elements defined as

$$M_{l_i,l_f}^{-\lambda-1} = \frac{1}{k_i k_f} \int_0^\infty F_{l_f}(k_f r)\, r^{-\lambda-1}\, F_{l_i}(k_i r)\, \mathrm{d}r. \tag{4}$$

Here, $F_l(kr)$ is the regular radial Coulomb function of angular momentum l. As here we only consider transitions from $j = 0$, the cross section for $j = 0 \to j' = \lambda$ is simply given by $\sigma_\lambda^{\mathrm{CB}}$.

The monopole ($\lambda = 0$) radial matrices can be obtained analytically (Alder *et al* 1956, van Regemorter 1960):

$$M_{l,l}^{-1} = \frac{2}{(k_i - k_f)^2} \frac{\mathrm{e}^{\pi\xi/2}}{\eta_i \eta_f} (-x^l) |\Gamma(l + 1 + \mathrm{i}\eta_i)| |\Gamma(l + 1 + \mathrm{i}\eta_f)|\, \mathrm{Re}(P) \tag{5}$$

with

$$P = \frac{\Gamma(-\mathrm{i}\xi)}{\Gamma(l + 1 - \mathrm{i}\eta_f)\Gamma(l + 1 + \mathrm{i}\eta_i)} t^{l+1+\mathrm{i}\xi/2} \mathcal{F}(l + 1 - \mathrm{i}\eta_i, l + 1 + \mathrm{i}\eta_f, 1 + \mathrm{i}\xi; t) \tag{6}$$

where $\eta = -1/k$, $\xi = \eta_f - \eta_i$, $x = -4\eta_i\eta_f/\xi^2$, $t = 1/(1 - x)$ and $\mathcal{F}$ is the complex hypergeometric function, which we evaluated using the subroutine HYPGEO (Press *et al* 1995). Only the first two monopoles need to be calculated in this way since the rest are related to them through a recurrence relation (see the appendix).

The dipole ($\lambda = 1$) radial matrices are obtained from the monopole ones (see the appendix). The quadrapole ($\lambda = 2$) radial matrices are also obtained from the monopole ones (see the appendix), except the elements $M_{0,2}^{-3}$ and $M_{2,0}^{-3}$ (Alder *et al* 1956, Chu 1975) which have to be calculated directly from (4). To do this we used the routine D01AKF (NAG 1996) to integrate numerically integral (4) using Coulomb functions evaluated by COULFG (Barnett 1982).

In the case of the dipole cross section σ_1^{CB}, the summation in (3) is evaluated exactly by closure Chu and Dalgarno (1974):

$$\sigma_1^{\mathrm{CB}}(j \to j') = \frac{3Q_1^2}{4\pi} \frac{2j' + 1}{k_i^2} \begin{pmatrix} j & j' & 1 \\ 0 & 0 & 0 \end{pmatrix} f_{E1}(\eta_i, \xi) \tag{7}$$

where

$$\begin{aligned} f_{E1}(\eta_i, \xi) = &-\frac{32\pi^3}{9} \frac{\eta_i\eta_f}{\xi} \frac{1}{\mathrm{e}^{2\pi\xi} - 1} \\ &\times \mathrm{Im}\left\{ \frac{1}{\eta_i} \mathcal{F}(\mathrm{i}\eta_i, \mathrm{i}\eta_i, 1 - \mathrm{i}\xi; \frac{1}{x}) \left[\mathcal{F}\left(1 - \mathrm{i}\eta_i, -\mathrm{i}\eta_i, 1 + \mathrm{i}\xi; \frac{1}{x}\right) \right.\right. \\ &\left.\left. + \mathrm{e}^{i\phi} \mathcal{F}\left(1 - \mathrm{i}\eta_f, -\mathrm{i}\eta_f, 1 - \mathrm{i}\xi; \frac{1}{x}\right) \right] + \eta_i \rightleftharpoons \eta_f \right\} \end{aligned} \tag{8}$$

where $\eta_i \rightleftharpoons \eta_f$ implies the addition of terms with η_i and η_f interchanged and

$$\phi = 2 \arg\left[\Gamma(\mathrm{i}\xi)\, \Gamma(\mathrm{i}\eta_i) / \Gamma(\mathrm{i}\eta_f)\right] + \xi \ln|x|. \tag{9}$$

Although the dipole cross section σ_1^{CB} is evaluated for an effectively infinite number of partial waves using (7), we still need (3) to calculate the low-partial-waves contribution and compare it with the same partial cross section obtained with the R-matrix models. Conversely, the quadrapole cross section σ_2^{CB} is only evaluated by direct summation using (3). Fortunately, the series converge very rapidly ($l_i, l_f < 10$) for the cases studied in this paper.

2.2. Rotational cross sections from body-frame T-matrices

We start with T-matrices for the electron scattering of molecules performed in the body frame (BF). In this work we do not consider vibrational or electronic excitation of the molecular ion, so the T-matrices elements are labelled according to the initial (l) and final (l') angular momentum of the projectile and its projection on the nuclear axis (Λ): $T^{\Lambda}_{l',l}$. To obtain rotational cross sections, it is necessary to transform these matrices into laboratory-frame (LAB) matrices, with total angular momentum J: $T^{J}_{j'l',jl}$. This is done by means of a simple rotational frame transformation (Morrison and Sun 1995):

$$T^{J}_{j'l',jl} \simeq \sum_{\Lambda=-l}^{l} A^{J\Lambda}_{j'l'}\, T^{\Lambda}_{l',l}\, A^{J\Lambda}_{jl} \tag{10}$$

with

$$A^{J\Lambda}_{jl} = \sqrt{\frac{2j+1}{2J+1}}\, C(j\ l\ J; 0\ \Lambda\ -\Lambda). \tag{11}$$

$C(\cdot)$ is a Clebsch–Gordan coefficient (Rose 1957).

Integrated rotational cross sections are obtained from (10)

$$\sigma^{\mathrm{RM}}(j \to j') = \frac{\pi}{k_i^2(2j+1)} \sum_{J=0}^{\infty} \sum_{l=|J-j|}^{J+j} \sum_{l'=|J-j'|}^{J+j'} (2J+1)|T^{J}_{j'l',jl}|^2. \tag{12}$$

In practice, it is necessary to truncate the partial-wave expansion to some finite $l_{\max}$ in any numerical treatment of the short-range interactions. Here $l_{\max} \leqslant 8$ is used. this means that it is unnecessary to consider values of J greater than 8. Contributions from higher partial waves are computed using the CB approximation through equation (13).

2.3. Final cross sections

The final cross section for the rotational excitation $j \to j'$ is obtained from the R-matrix cross section and completed with the CB ones:

$$\sigma(j \to j') = \sigma^{\mathrm{RM}}(j \to j') + \sigma^{\mathrm{CB}}_{\lambda} - \sigma^{\mathrm{PCB}}_{\lambda} \tag{13}$$

where we call σ^{PCB} to the 'partial' CB cross section calculated using a few partial waves in (3) ($l_i, l_f \leqslant l_{\max}$).

In practice, for $\lambda > 1$, the two CB terms almost cancel because equation (3) converges rapidly. In these cases we use

$$\sigma(j \to j') = \sigma^{\mathrm{RM}}(j \to j'). \tag{14}$$

2.4. Threshold effects

The cross sections discussed above are obtained using theoretical treatments of the collision event known as adiabatic nuclear rotation (ANR). It assumes that the rotational states of the target are degenerate. This assumption leads to a problem in these cross sections: they do not go to zero at threshold. The simplest way of correcting this feature is to force the cross section at threshold to zero using a kinematic ratio (Chandra and Temkin 1976, Morrison and Sun 1995):

$$\sigma^{\mathrm{tc}}(j \to j') = \frac{k_f}{k_i}\, \sigma(j \to j'). \tag{15}$$

3. Generation of T-matrices

In the calculation of the BF T-matrices, we employ the UK molecular R-matrix package (Gillan *et al* 1995). Three different models are explored in this work, details of which are given below.

3.1. Fixed-nuclei model (FN)

The calculations are performed at a given internuclear distance (R). According to the R-matrix method, space is separated into two parts by a sphere centred in the centre of mass of the molecular ion. In the inner region, the wavefunction is expanded in a close-coupling fashion as

$$\Psi_k = \mathcal{A} \sum_{i,j} a_{i,j,k} \Phi_i F_{i,j} + \sum_i b_{i,k} \Xi_i \tag{16}$$

where $\mathcal{A}$ is the antisymmetrization operator, Φ_i are N-electron target wavefunctions, $F_{i,j}$ are continuum orbitals and Ξ_i are $(N+1)$-electron, two-centre, L^2 functions constructed from the target occupied and virtual molecular orbitals. In this work the target wavefunctions, Φ_i, are expressed as phase corrected (Tennyson 1997) configuration-interaction (CI) expansions based on the use of complete active space (CAS) wavefunctions.

Calculations using this model were performed at the equilibrium distance of the ions and a number of internuclear distances to produce T-matrices ($^{\mathrm{FN}}T^{\Lambda}_{l',l}$) necessary for the adiabatic model.

3.2. Adiabatic model

The adiabatic T-matrices were obtained by vibrationally averaging the fixed-nuclei T-matrices (Chase 1956):

$$^{\mathrm{A}}T^{\Lambda}_{l'v',lv} = \int \chi_{v'}(R)\, ^{\mathrm{FN}}T^{\Lambda}_{l',l}(R)\, \chi_v(R)\, \mathrm{d}R \tag{17}$$

where χ_v are vibrational wavefunctions, the calculation of which is detailed below.

3.3. Non-adiabatic model

Non-adiabatic effects due to the vibrational motion of the nuclei are considered via a non-adiabatic approximation (Gillan *et al* 1987) introduced by Schneider *et al* (1979). The implementation of this approximation divides internuclear coordinate space with a region defined by $A_{\mathrm{in}} \leqslant R \leqslant A_{\mathrm{out}}$, outside which the vibrational functions (χ_v) have negligible amplitude.

The eigenfunctions in this model are obtained by diagonalizing a Hamiltonian that includes the nuclear kinetic energy operator in the basis

$$\theta_k = \sum_{ij} \Psi_i(R)\, \xi_j(R)\, \gamma_{ijk} \tag{18}$$

where Ψ_i is the wavefunction given in (16) and ξ_j a set of Legendre polynomials to describe the nuclear motion. T-matrices with this model ($^{\mathrm{NA}}T^{\Lambda}_{l'v',lv}$) are obtained when matching, at the hypersphere surface, the inner region wavefunction with the outer region one:

$$\theta = \sum_{ijv} \Phi_i\, r_{N+1}^{-1}\, F_{iv}(r_{N+1})\, Y_{l_j m_j}(\hat{\boldsymbol{r}}_{N+1})\, \chi_{iv}(R) \tag{19}$$

where Φ_i are the target electronic channels, χ_{iv} the target vibrational channels and F_{iv} monoelectronic radial functions.

Both the adiabatic and non-adiabatic T-matrices are obtained vibrationally resolved. As in this work vibrational excitation is not considered, the label v is dropped below.

3.4. HeH^+ wavefunctions

HeH^+ wavefunctions were taken from the calculations of Sarpal *et al* (1991a, b), where full details can be found. In the inner region of 10 a_0, Ψ_k was constructed using the three lowest HeH^+ states (which were CI expansions), correlation and polarization terms. The continuum orbitals were calculated numerically using the isotropic part of the SCF potential and included all of them with $l \leqslant 5$, $m \leqslant 3$ and energy below 10 Ryd.

The fixed-nuclei wavefunctions and T-matrices were obtained at 13 internuclear lengths in the range $A_{\text{in}} = 1.0$ and $A_{\text{out}} = 4.0$ a_0 (including equilibrium at $R_{\text{e}} = 1.455$ a_0). The potential energy curve for the HeH^+ ground state thus obtained was fitted to a Morse potential and its first six eigenfunctions used as vibrational states in the outer region calculations of the non-adiabatic T-matrices. Furthermore, the ground state dipole and quadrapole moments were retained in the outer region potential.

T-matrices were obtained for $\Lambda = 0, 1, 2, 3$ and included terms with $l, l' \leqslant 5$. Values used for the CB calculations were $B_{\text{e}} = 33.47$ cm^{-1}, $Q_1 = 1.66$ Debye and $Q_2 = -1.398$ au.

3.5. NO^+ wavefunctions

NO^+ wavefunctions were taken from the calculations of Rabadán and Tennyson (1997) and Rabadán *et al* (1998a), where full details can be found. An inner region of 15 a_0 for the electronic coordinates was used in the calculation of the fixed-nuclei wavefunctions Ψ_k (16). These were constructed using the 12 lowest NO^+ states Φ_i, which in turn were represented using a CI expansion. Correlation and orthogonality relaxing effects were added to the CI expansion using the second sum in (16). The continuum was represented using $l \leqslant 6 + m, m \leqslant 2$ (60σ, 57π, 54δ) numerical functions obtained in an isotropic Coulomb potential.

The functions Ψ_k and fixed-nuclei T-matrices were calculated for 14 internuclear distances between $A_{\text{in}} = 1.606$ and $A_{\text{out}} = 2.835$ a_0 (including the equilibrium one at $R_{\text{e}} = 2.003$ a_0). Outer region calculations retained all 12 target states explicitly, and all diagonal and off-diagonal terms of the dipole and quadruple potentials.

The vibrational wavefunctions used in (17) and (19) were calculated by numerically solving the Schrödinger equation (Leroy 1996) in the *ab initio* $NO^+(X\ ^1\Sigma^+)$ calculated in Rabadán and Tennyson (1997). Ten vibrational states and only the NO^+ electronic ground state were used in the outer region calculations of the non-adiabatic T-matrices.

T-matrices for $\Lambda = 0, 1, 2$ were obtained and six partial waves were considered for each symmetry. Values used for the CB calculations were $B_{\text{e}} = 2.002$ cm^{-1}, $Q_1 = 0.257$ Debye and $Q_2 = 0.379$ au.

4. Results and discussion

Rotational excitation cross sections were obtained for a number of models for both HeH^+ and NO^+ target ions. Pure CB approximation calculations were compared with ones where the short-range interaction are treated using the fixed-nuclei approximation, where

vibrational motion was treated adiabatically or where a complete non-adiabatic treatment of the vibrational motion was performed. As the treatment of short-range interactions was only possible, or indeed necessary, for low partial waves, in cases where $\Delta j \leqslant 2$ the effect of treating higher partial waves via the CB approximation was also considered. In particular, we complete the R-matrix six partial-waves cross section for each molecule with the CB cross section using equation (13). This completion is, effectively, to an infinite number of partial waves for dipole transitions and 10 partial waves for quadrupole ones.

Use of the threshold correction to the ANR cross sections was also tested in each case. It is not actually necessary to present results for all these models as, for example, all treatments of the electronic and vibrational wavefunctions showed the same behaviour with and without the threshold correction in (15). Only the important results are given below. For $\Delta j \leqslant 2$, results are considered for each target in turn. Results for $\Delta j > 2$ are considered afterwards.

4.1. HeH^+

Figure 1 summarizes the results of $\Delta j = 1$ calculations on HeH^+. As HeH^+ has a large dipole, the long-range effects as given by the CB approximation, are only slowly convergent. Comparisons showed that these long-range contributions were greater in magnitude than those given by the low partial waves in the various models which included short-range interactions. As these low partial waves contribute little to the CB calculations, the net

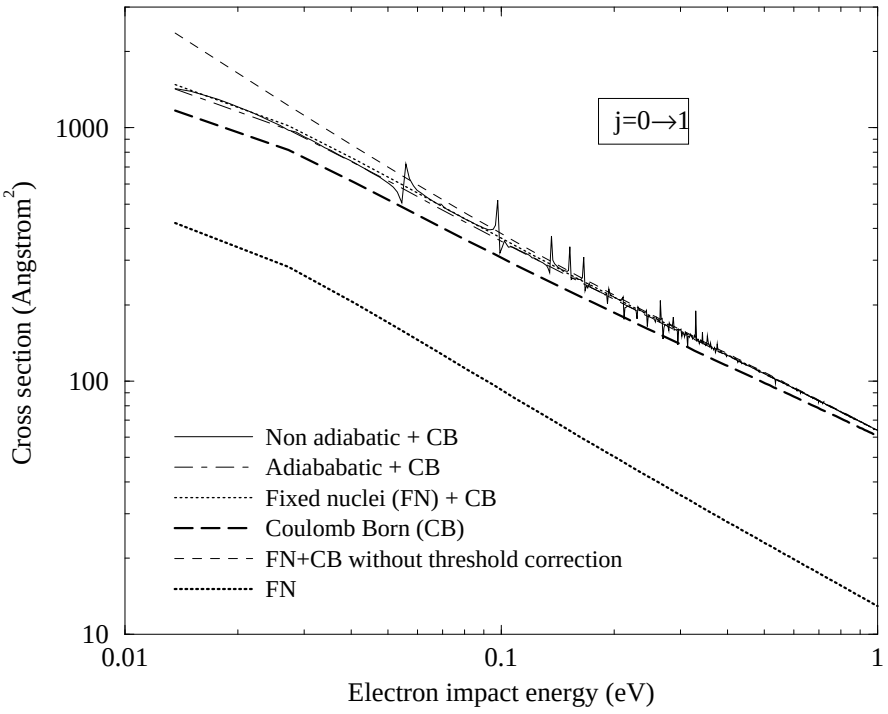

Figure 1. Rotational excitation cross section of $HeH^+(j = 0 \rightarrow 1)$ by electron impact. Theoretical models are indicated in the graph. In the key, '+CB' indicates that the corresponding R-matrix model has been completed with high-l CB cross sections using equation (13).

effect of a short-range model augmented by CB T-matrices is to give cross sections slightly larger than the pure CB calculation.

Comparison of the three methods of treating nuclear motion, fixed-nuclei, adiabatic nuclei and non-adiabatic, show that all three models give very similar cross sections at all energies. The only significant departure from this is the complicated structure introduced when the vibrational motion is treated non-adiabatically. In this case there are many narrow resonances corresponding to vibrationally excited states of bound HeH Rydberg states (Sarpal *et al* 1991b). However, although these resonances undoubtedly complicate the structure of the cross section as a function of energy, they do not, if one considers the integral over the resonance region, appear to change the cross section significantly.

Figure 1 includes results of the FN model cross section with and without the threshold correction. This approximation only leads to a significant difference in the cross section below 0.2 eV, but leads to a substantial difference at low energies. As this correction is independent of the model, this finding is true for all models.

Figure 2 gives results for $\Delta j = 2$ transitions for HeH^+. As HeH^+ has a large dipole and all previous treatments of this system have assumed that only $\Delta j = 1$ transitions need to be considered, we were surprised that the $\Delta j = 2$ CB cross sections proved to be somewhat larger than the $\Delta j = 1$ CB cross sections presented in figure 1. However, the $\Delta j = 2$ CB model is somewhat different to the $\Delta j = 1$ one in that it is entirely dominated by low partial waves. This means that the results obtained using the frame transformation methods were essentially unaltered by augmenting them with CB calculations for higher partial

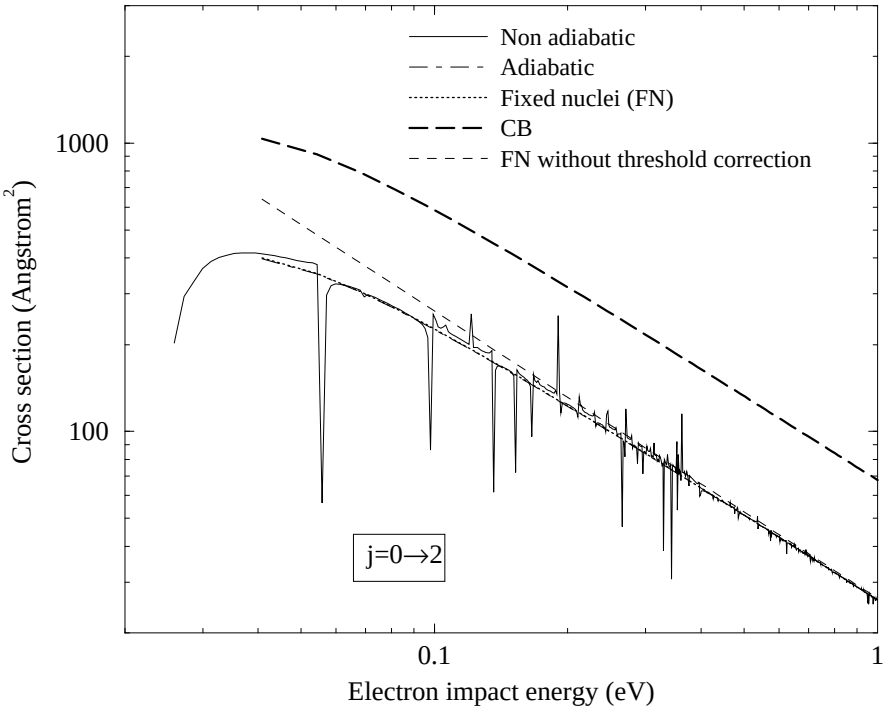

Figure 2. Rotational excitation cross section of $HeH^+(j = 0 \rightarrow 2)$ by electron impact. Theoretical models are indicated in the graph.

waves. Furthermore, the frame transformation calculations show that the CB approximation substantially overestimates the $\Delta j = 2$ cross sections.

Again the only significant difference between the three treatments of vibrational motion is the resonance structure introduced in the non-adiabatic calculation. For the $\Delta j = 2$ case, this structure appears to be more pronounced, a result of the cross section being dominated by a few, low partial waves, and the structure appearing more as windows. The latter effect may, at least in part, be due to our choice of energy grid.

Not surprisingly, given that the $\Delta j = 2$ excitation threshold is three times that for $\Delta j = 1$, the threshold-corrected calculations differ even more markedly at low energy than they do in the $\Delta j = 1$ case.

4.2. NO^+

There are some important differences between our results for NO^+ and HeH^+; an obvious one being that while rotational excitation threshold effects, as manifested by the use of the threshold-corrected model, are important for HeH^+, no such behaviour was found for NO^+. The lower rotational excitation energy of NO^+ means that for the electron collision energies considered here ($\geqslant$0.1 eV), calculations with or without the correction were indistinguishable.

NO^+ has a smaller dipole than HeH^+. This means that the $\Delta j = 1$ cross sections, see figure 3, are significantly (about a factor of ten) smaller and are dominated by short-range

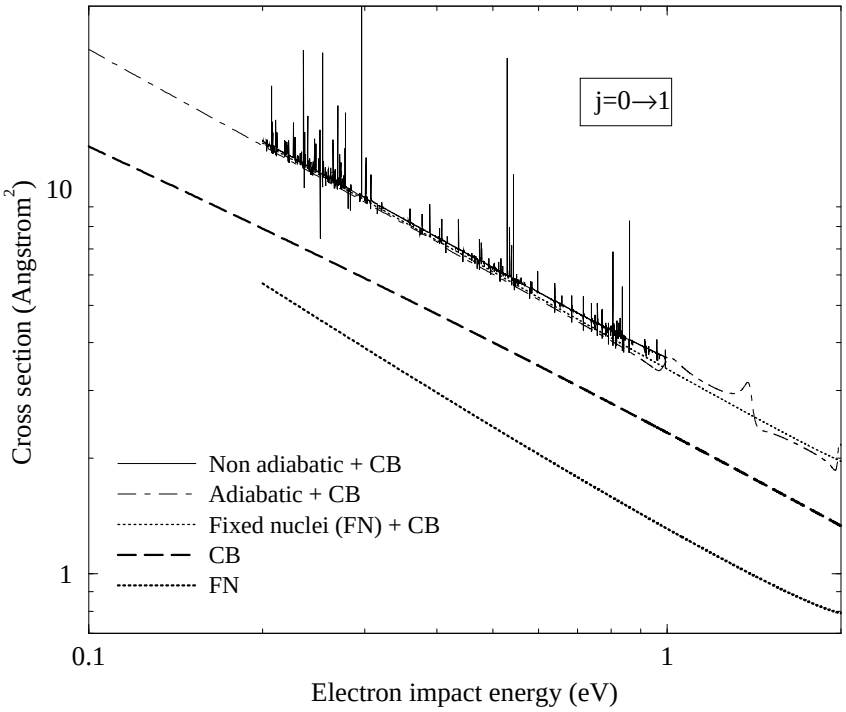

Figure 3. Rotational excitation cross section of $NO^+(j = 0 \rightarrow 1)$ by electron impact. Theoretical models are indicated in the graph. In the key, '+CB' indicates that the corresponding *R*-matrix model has been completed with high-*l* CB cross sections using equation (13).

effects. A pure CB calculation underestimates the cross section by about a factor of nearly two. However, as in HeH^+, it was still necessary to augment the low-partial-wave models with CB results for the higher partial waves to obtain converged cross sections.

For NO^+ there are differences between the various vibrational treatments. In particular, the non-adiabatic treatment gives a higher 'background' $\Delta j = 1$ cross section augmented by an even more complicated resonance structure than in the HeH^+ case. Again this resonance structure arises from autoionizing levels of vibrationally excited Rydberg states; a detailed theoretical analysis has been presented elsewhere (Rabadán *et al* 1998a). The increase in complexity is due to the closer vibrational spacing found in NO^+. Furthermore, the fixed-nuclei and adiabatic models do not agree at higher energies. However, the structure shown in the adiabatic model at these energies is consequence of the incorrect treatment of intruder states of NO, which appear at these energies (Rabadán and Tennyson 1997, 1998b). This model is probably best avoided for rotational excitation calculations.

Figure 4 shows that for NO^+, $\Delta j = 2$ excitation is more likely for all models than $\Delta j = 1$. It has often been noted that NO^+, which is isoelectronic with N_2, is quasi-homonuclear (Kaufmann 1991). For a homonuclear diatomic, excitations with Δj odd are symmetry forbidden.

Like HeH^+, the $\Delta j = 2$ cross section, in all models, arises purely from the low partial waves. Unlike HeH^+, the CB model underestimates the cross section significantly, by a factor of about 4. Our best models suggest that for NO^+ electron impact is about five times more likely to lead to $\Delta j = 2$ than $\Delta j = 1$ at energies above the $\Delta j = 2$ threshold.

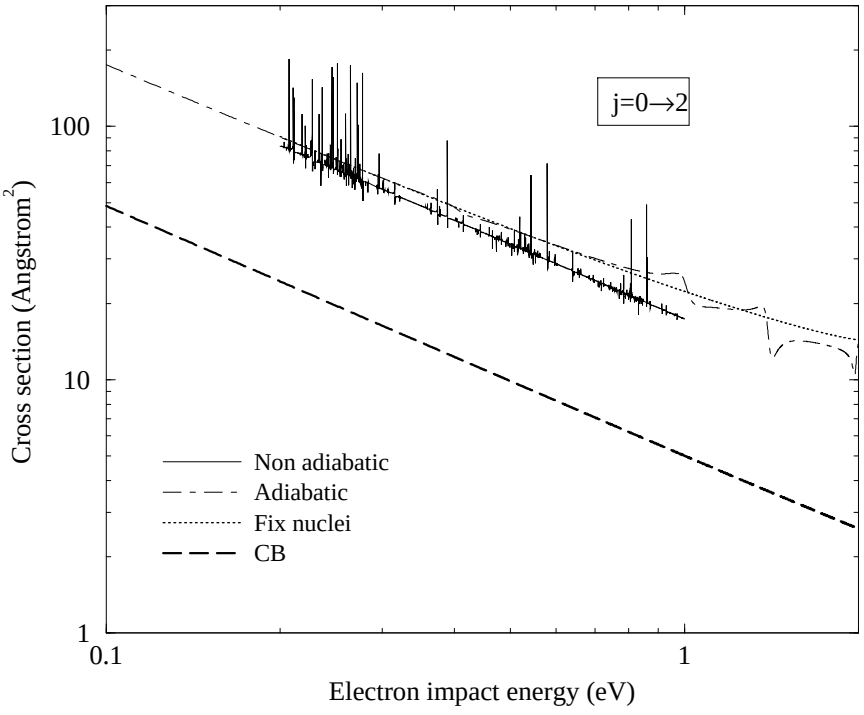

Figure 4. Rotational excitation cross section of $NO^+(j = 0 \rightarrow 2)$ by electron impact. Theoretical models are indicated in the graph.

4.3. Higher rotational excitation

As $\Delta j = 2$ excitation cross sections appear larger than had been previously anticipated, it is necessary to consider electron-impact excitation to even higher rotational states. Calculations were performed for $\Delta j = 3$ and 4 using the fixed-nuclei approximation and, for HeH^+, the threshold-corrected model. As none of our calculations included, or indeed have ever included, multipole moments higher than quadrapole, there can be no long-range contribution to these higher cross sections. It was therefore not necessary to consider the CB model or the effects of higher partial waves. This is consistent with the very rapid convergence obtained for the $\Delta j = 2$ considered above.

Figure 5 gives a comparison of $\Delta j = 1, 2, 3, 4$ excitation cross sections for both HeH^+ and NO^+. For HeH^+ the $\Delta j = 3$ and 4 cross sections are small and can probably be safely ignored. This is not so for NO^+, where the $\Delta j = 4$ cross section is significantly larger than the $\Delta j = 1$ one, which up until now has been assumed to be totally dominant!

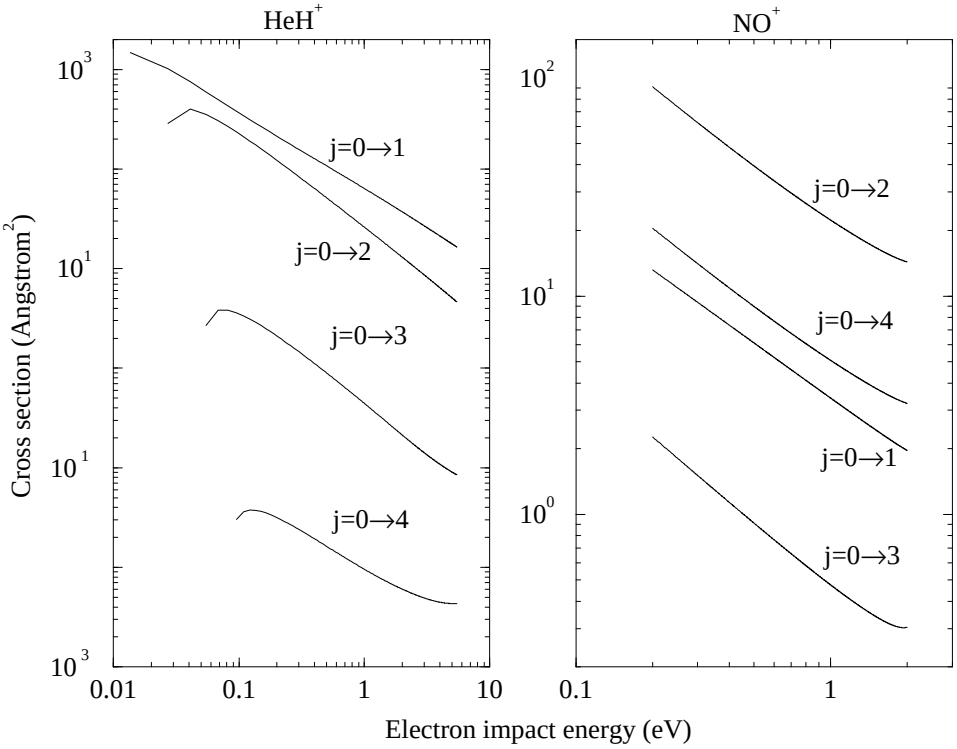

Figure 5. Rotational excitation of NO^+ and HeH^+ by electron impact.

5. Conclusions

We have performed a series of calculations for electron-impact rotational excitation of the molecular ions HeH^+ and NO^+ using different models. Our calculations show that the widespread uncritical use of the dipole Coulomb–Born model is dangerous as short-range interactions can significantly modify the cross sections and, even more importantly, it is unsafe to assume that only $\Delta j = 1$ excitations need to be considered. The latter finding is

likely to be particularly important for observing models of diffuse molecular plasmas such as those found in the interstellar medium.

For light molecules, such as HeH^+, threshold effects can be important. Indeed rotational excitation rates which neglect threshold effects will be significantly overestimated (Rabadán *et al* 1998b). Conversely our findings suggest that detailed treatments of vibrational motion are probably unnecessary to obtain reliable rotational excitation rates. For this purpose we would advocate the use of fixed-nuclei calculations which include a full treatment of short-range interactions. For $\Delta j = 1$, these cross sections should be augmented by Coulomb–Born calculations for higher partial waves. For light molecular ions the threshold-corrected rotational excitations (Chandra and Temkin 1976) should be used to allow for threshold effects. ROTIONS, a general computer program developed for performing the calculations reported here, has been made generally available (Rabadán and Tennyson 1998a).

Acknowledgments

We thank Peter Storey and Xiaowei Liu for helpful discussions. This work was supported by the UK Engineering and Physical Sciences Research Council and Particle Physics and Astronomy Research Council. BKS's work was supported by a Sir James Knott Fellowship.

Appendix. Recurrences and relations between radial matrix terms

Monopole terms

The recurrence relation to obtain monopole matrix elements from other monopole terms is given by (Alder *et al* 1956)

$$M^{-1}_{l+1,l+1} = \frac{1}{2l|l+1+\mathrm{i}\eta_i||l+1+\mathrm{i}\eta_f|} \times \left\{ (2l+1)\left[\frac{\eta_i^2+\eta_f^2}{\eta_i\eta_f} l(l+1) + 2\eta_i\eta_f\right] M^{-1}_{l,l} - (2l+2)|l+\mathrm{i}\eta_i||l+\mathrm{i}\eta_f| M^{-1}_{l-1,l-1} \right\}. \tag{A1}$$

Dipole terms

Dipole matrix elements are obtained from monopole ones with the relation (Alder *et al* 1956)

$$M^{-2}_{l,l+1} = \frac{k_f}{l+1}|l+1+\mathrm{i}\eta_f| M^{-1}_{l,l} - \frac{k_i}{l+1}|l+1+\mathrm{i}\eta_i| M^{-1}_{l+1,l+1}. \tag{A2}$$

Quadrapole terms

Quadrapole radial matrices are related to the monopole ones by (Alder *et al* 1956)

$$M^{-3}_{l,l+2} = f(l)\left(\frac{M^{-3}_{l-1,l+1}}{f(l-1)} + \frac{A(l-1)}{f(l)}\right) \tag{A3}$$

with

$$f(l) = \left(\frac{\eta_f}{\eta_i}\right)^l \left|\frac{\Gamma(l+1+\mathrm{i}\eta_i)}{\Gamma(l+3+\mathrm{i}\eta_f)}\right| \tag{A4}$$

$$A(l) = \frac{k_i^2 - k_f^2}{4(l+1)|l+2+\mathrm{i}\eta_f||l+3+\mathrm{i}\eta_f|}\frac{1}{\eta_i^2} \times\left\{[2\eta_i^2\eta_f^2 + \eta_f^2(l+1)(2l+3) - \eta_i^2(l+1)]M_{l+1,l+1}^{-1} -2\eta_i\eta_f|l+1+\mathrm{i}\eta_i||l+1+\mathrm{i}\eta_f|M_{l,l}^{-1}\right\}. \tag{A5}$$

Diagonal quadrapole terms are obtained from off-diagonal terms (Alder *et al* 1956):

$$yM_{l,l}^{-3} = y_1M_{l,l+2}^{-3} + y_2M_{l-1,l+1}^{-3} + y_3M_{l+2,l}^{-3} + y_4M_{l+1,l-1}^{-3} \tag{A6}$$

with

$$y = \frac{l(l+1)}{3}(\eta_f^2 - \eta_i^2)$$
$$y_1 = -\eta_i^2|l+1+\mathrm{i}\eta_f||l+2+\mathrm{i}\eta_f|$$
$$y_2 = \eta_i\eta_f\frac{2l+3}{2l+1}|l+\mathrm{i}\eta_i||l+1+\mathrm{i}\eta_f|$$
$$y_3 = \eta_f^2|l+1+\mathrm{i}\eta_i||l+2+\mathrm{i}\eta_i|$$
$$y_4 = -\eta_i\eta_f\frac{2l+3}{2l+1}|l+\mathrm{i}\eta_f||l+1+\mathrm{i}\eta_i|.$$

The $M_{l+1,l}^{-2}$ and $M_{l+2,l}^{-3}$ terms are obtained from (A2) and (A3), respectively, by interchanging η_i and η_f.

References

Alder K, Bohr A, Huss T, Mottelson B and Winther A 1956 *Rev. Mod. Phys.* **28** 432

Barnett A R 1982 *Comput. Phys. Commun.* **27** 147–66

Cecchi-Pestellini C and Dalgarno A 1993 *Astrophys. J.* **413** 611

Cernicharo J, Liu X-W, González-Alonso E, Cox P, Barlow M J, Lim T and Swinyard B M 1997 *Astrophys. J.* **483** L65–8

Chandra N and Temkin A 1976 *Phys. Rev.* A **13** 188

Chase D M 1956 *Phys. Rev.* **104** 838

Chu S-I 1975 *Phys. Rev.* A **12** 396–405

Chu S-I and Dalgarno A 1974 *Phys. Rev.* A **10** 788–92

Dickinson A S and Flower D R 1981 *Mon. Not. R. Astron. Soc.* **196** 297

Dickinson A S and Muñoz J M 1977 *J. Phys. B: At. Mol. Phys.* **10** 3151–63

Flower D R 1979 *Astron. Astrophys.* **73** 237–9

Gillan C J, Nagy O, Burke P G, Morgan L A and Noble C J 1987 *J. Phys. B: At. Mol. Phys.* **20** 4585

Gillan C J, Tennyson J and Burke P G 1995 *Computational Methods for Electron Molecule Collisions* ed W M Huo and F A Gianturco (New York: Plenum) pp 239–52

Kaufmann K 1991 *J. Phys. B: At. Mol. Opt. Phys.* **24** 2277

Lane N F 1980 *Rev. Mod. Phys.* **52** 29

Leroy R J 1996 *University of Waterloo Chemical Physics Research Report* CP-555R 1–11

Liu X-W *et al* 1997 *Mon. Not. R. Astron. Soc.* **290** L71–5

Morrison M A and Sun W 1995 *Computational Methods for Electron Molecule Collisions* ed W M Huo and F A Gianturco (New York: Plenum) pp 131–90

NAG Fortran Library 1996 The Numerical Algorithms Group Ltd, Oxford

Neufeld D A and Dalgarno A 1994 *Phys. Rev.* A **40** 633

Press W H, Flannery B P, Teukilsky S A and Vetterling W T 1995 *Numerical Recipes in Fortran* (Cambridge: Cambridge University Press)

Rabadán I and Tennyson J 1997 *J. Phys. B: At. Mol. Opt. Phys.* **30** 1975–88
——1998a *Comput. Phys. Commun.* submitted
——1998b *J. Phys. B: At. Mol. Opt. Phys.* to be submitted
Rabadán I, Morgan L A and Tennyson J 1998a *Chem. Phys. Lett.* **285** 105–13
Rabadán I, Sarpal B K and Tennyson J 1998b *Mon. Not. R. Astron. Soc.* in press
Roberge W and Dalgarno A 1982 *Astrophys. J.* **255** 489
Rose M E 1957 *Elementary Theory of Angular Momentum* (Wiley: New York)
Sarpal B K, Branchett S E, Tennyson J and Morgan L A 1991a *J. Phys. B: At. Mol. Opt. Phys.* **24** 3685–99
Sarpal B K, Tennyson J and Morgan L A 1991b *J. Phys. B: At. Mol. Opt. Phys.* **24** 1851–66
Schneider B I, Le Dourneuf M and Burke P G 1979 *J. Phys. B: At. Mol. Phys.* **40** L365
Tennyson J 1997 *Comput. Phys. Commun.* **100** 26
Thümmel H T, Nesbet R K and Peyerimhoff S D 1993 *J. Phys. B: At. Mol. Opt. Phys.* **26** 1233–51
van Regemorter H 1960 *Mon. Not. R. Astron. Soc.* **121** 213–31